Hindawi Publishing Corporation
International Journal of Antennas and Propagation
Volume 2013, Article ID 602716, 9 pages
http://dx.doi.org/10.1155/2013/602716

Research Article

Array-Based Ultrawideband through-Wall Radar: Prediction and Assessment of Real Radar Abilities

Nadia Maaref and Patrick Millot

DEMR (Département d'Électromagnétisme et Radar), Onera (The French Aerospace Lab), 31055 Toulouse, France

Correspondence should be addressed to Nadia Maaref; nadia.maaref@onera.fr

Received 4 October 2012; Revised 6 December 2012; Accepted 17 December 2012

Academic Editor: Matteo Pastorino

This paper deals with a new through-the-wall (TTW) radar demonstrator for the detection and the localisation of people in a room (in a noncooperative way) with the radar situated outside but in the vicinity of the first wall. After modelling the propagation through various walls and quantifying the backscattering by the human body, an analysis of the technical considerations which aims at defining the radar design is presented. Finally, an ultrawideband (UWB) frequency modulated continuous wave (FMCW) radar is proposed, designed, and implemented. Some representative trials show that this radar is able to localise and track moving people behind a wall in real time.

1. Introduction

Through-the-wall (TTW) radar technique addresses electromagnetic "vision" behind walls in order to detect, count, and localise people inside a building. Considering one by one these three objectives: detect, count, and localise, it is possible to situate our work among the various researches that are ongoing in the TTW radar field.

In order to detect one or more persons in a room, it is necessary to take into account the fact that these people move. In fact, the radar return coming from the human body is not high enough compared to the backscattering of the indoor environment to ensure detection. So that, Doppler effect has been used historically to detect motion through walls [1]. Nevertheless, Doppler radar has also some drawbacks. The first one is its high sensitivity to all kinds of motions bringing false alarms. The second one is that target localisation and Doppler filtering seems incompatible. This is why emphasis was made on imaging radar with the ability to count and localise targets.

Small TTW radars based on the technology of UWB pulses appeared since the 2000s. The famous ones are Radarvision and then Xaver by CAMERO. There is no publication about them in the open literature. Besides, some radar and signal processing specialized laboratories have studied UWB radar imaging or SAR imaging applied to through-wall vision [2, 3].

The work presented here gives the last advances from our laboratory in the "see-through" radar topic. It aims at giving a global approach of the TTW radar detection. It shows step by step the design process after radar modelling: from theoretical background to radar realization followed by experimental assessment. In Section 2, the through-the-wall propagation physics has been studied by simulation and also assessed by measurements. Then, in Section 3, the backscattering strength of the human body is quantified in an anechoic chamber with various people under test. Section 4 is centred on an analysis of technical considerations which aims at defining the best radar design. And finally, Sections 5 and 6 present the radar implementation and a trial of people detection and localization through a wall.

2. Through-the-Wall Propagation

2.1. Electromagnetic Through-the-Wall Propagation Modelling. In through-the-wall radar, wave propagation through wall materials has a great influence on the radar concept because it can be responsible of large wave attenuation.

When studying through-the-wall radar, one must predict the influence of walls on radar signals. To achieve this goal,

we propose to use in-depth EM wall modelling to evaluate wall responses to radar waves. We have especially investigated propagation through walls made of brick, cinder block, or concrete.

First, a simple 1D simplified multilayer electromagnetic model is considered. Knowing the relative permittivity of a given material, its transmission and reflection coefficients through it can be computed [4]. Let us consider two different types of walls: a 20 cm thick brick wall with four air gaps and a 20 cm thick solid concrete wall. Time domain representations have also been obtained by inverse Fourier transform of frequency computations from 1 GHz to 5 GHz. Time delays are converted to equivalent distances using the electromagnetic wave speed in air.

Dielectric properties of building materials can be found in the open literature. For the simulations, brick wall has been modelled by a material whose relative permittivity is $\varepsilon_r = 5 - j \cdot 0.3$ [5] and concrete wall has been modelled by a bulk material whose relative permittivity is $\varepsilon_r = 8 - j \cdot 0.7$ [6].

Brick wall transmission shows strong frequency dependence (Figure 1). Mean transmission losses are about 15 dB but maximum losses of 25 dB can be observed. The round trip transmission loss of 30 dB may have a strong impact on the radar power budget, as it restricts the TTW radar detection range. The large uncertainties on the predicted value of the transmission require us to maintain a high dynamic range (here 20 dB) for the detector threshold voltage.

As a consequence of phase dispersion, the major peak of the time response is followed by a side-lobe "clutter" not localized on the wall in time domain. This clutter level decreases with time delay and is less than 30 dB under maximum for distances larger than 1 m and 70 dB for distances larger than 3 m. This parasitic signal may impede human detection when the radar target is close to the wall because it may conceal a target.

The solid concrete slab presents a different electromagnetic response (Figure 2). The transmission coefficient decreases continuously from −10 dB to −50 dB over the whole frequency bandwidth. Time domain transmission shows a first peak followed by some peaks at much lower levels. Due to wave absorption through concrete, internal ringing is more attenuated so the concrete wall brings less "clutter." Then, for a transmission criterion, one needs to use also frequencies as low as 1 GHz.

The 1D electromagnetic model is an analytical and straight-forward method based on the modelling of wall structure by a succession of dielectric layers. In order to consider the exact internal structure of a wall (real walls are nonhomogeneous), we have chosen to model in a second time using a full wave simulator: the Finite Difference Time Domain (FDTD) method [7]. Besides the problem to represent the scene (by a duly informed mesh), this method is known to be quite simple and robust for computing but time consuming.

Let us compare between 1D and 3D modelling of the transmission through a brick wall. We consider a given brick, used in France for building private houses, composed of four air gaps (alveoli). The result of the simulation made by FDTD is superposed to the one obtained with the 1D electromagnetic model presented previously (see Figure 3).

As one can see, taking into account the complexity of the structure brings some additional fluctuations in frequency on the computed transmission coefficient.

This is certainly due to the multiple reflections inside the brick (some kinds of dielectric cavity mode resonances). However, the general shape remains the same with an important attenuation of about 20 dB around 2.2 GHz.

2.2. Transmission Measurements and Comparison with the Model. Transmission measurements have been performed in a house under construction in order to compare simulation results to real data. This measurement is the wall transfer function measurement in situ. The antennas face one another with the wall between them and are fixed at 1.5 m above the soil. The distance from each antenna to the wall is 1 m. The wall is made of 20 cm brick (including three 5 cm thick air gaps), air (3 cm), rock-wool (8.5 cm), and plasterboard (7 mm).

Frequency measurements in transmission (S_{12}) have been performed using a Vector Network Analyzer. Let $V_{\text{ref}}(F)$ and $V_{\text{wall}}(F)$ be respectively the recorded values with and without the wall. The insertion transfer function is simply given by the following complex ratio:

$$T(F) = \frac{V_{\text{wall}}(F)}{V_{\text{ref}}(F)}. \quad (1)$$

In order to model this wall, the relative mean permittivity of brick, that is, 5–0.3 j, has been chosen. The influence of rock-wool (close to air) and plasterboard (thickness 7 mm) is quite negligible. In Figure 4, one can see the result of the modelling (dashed curve) and the one from the measurement (full line curve). The two curves are rather similar up to 2.5 GHz with a mean gap of 5 dB. Between 2.5 and 3.5 GHz, the gap between measurement and simulation expands to reach a maximum value of 25 dB. And, finally, from 3.5 GHz, the two curves tend to be similar again with a max gap of 15 dB. This comparison shows that there are discrepancies for some frequencies between simulation and measurement (due to the errors brought by model assumptions). However, the model predicts rather well the transmission behaviour with respect to the frequency (strong attenuation between 2 and 3 GHz).

We have also considered the case of cinder blocks wall which is also widely used for large buildings. The wall under test is made of 20 cm thick hollow concrete elements. The measurement method is the same as previously, but, this time, several measurements all along the wall have been made in order to increase position diversity in measurements. Figure 5 (full line curve) presents a typical transfer function measured when the two antennas faced together. The amplitude fluctuates between −6 dB and −50 dB.

This measurement is compared with an FDTD simulation result. The adopted relative permittivity of concrete blocks is 6. Each block is 50 cm × 20 cm × 20 cm. Air gaps are 7.5 cm width in the direction of the wave vector. A quite similar behaviour (dash line curve) can be seen for both simulation

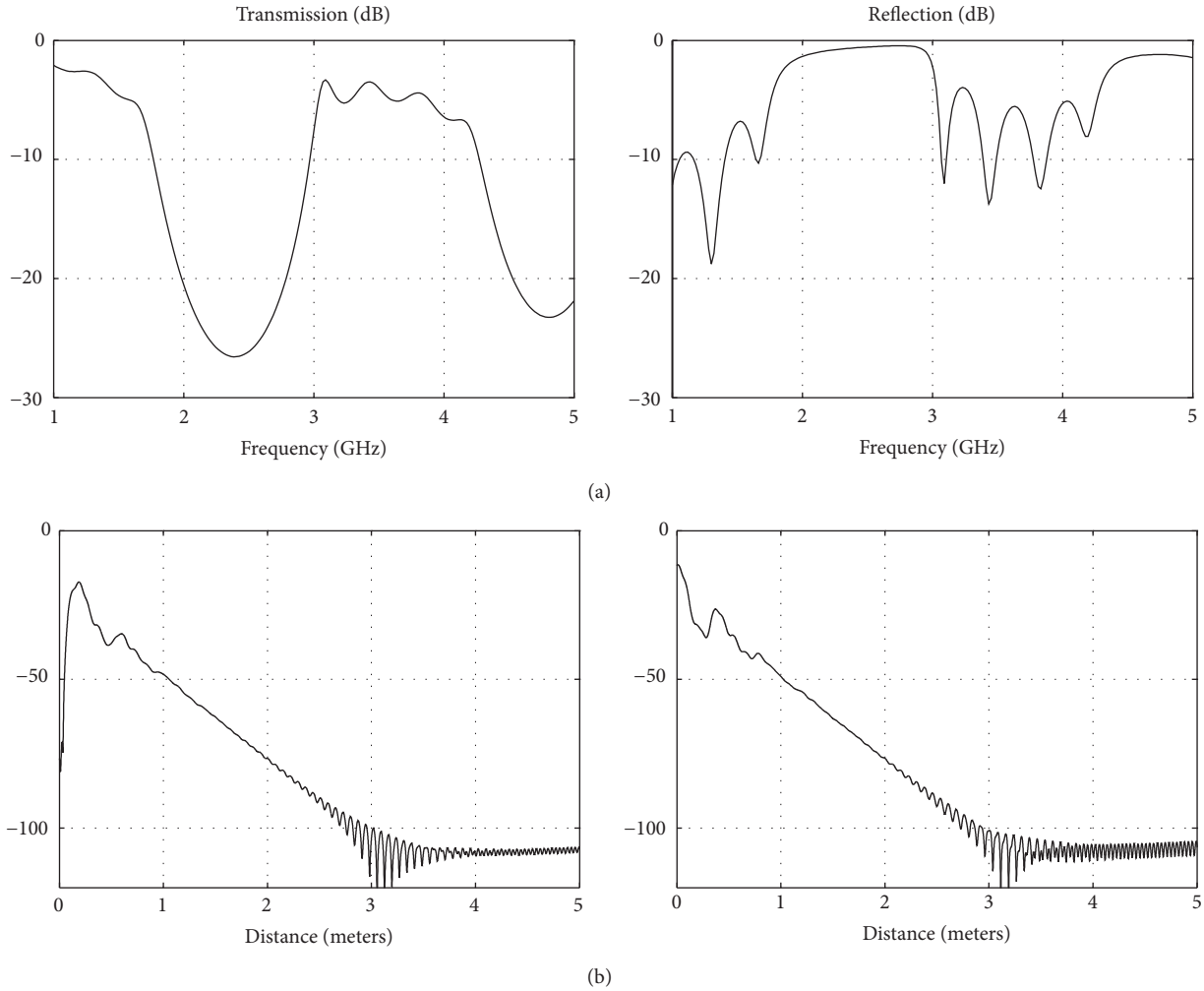

Figure 1: 20 cm brick wall transmission and reflection coefficient in frequency domain (a) and in time domain (b).

and measurement at the lower part of the frequency bandwidth (around 1 GHz). Note that the wall transfer function depends strongly on the position of the electromagnetic sources used for the simulation, a fact that is confirmed by the measurement.

In conclusion, we can assert that both simulations and measurements have shown a strong signal attenuation increasing with the frequency in the case of homogeneous structures (like solid concrete). In the case of "hollow" walls, signal attenuation strongly depends on the considered wall structure (number and size of air gaps, etc.). For this kind of walls, the time response presents a "tail" that could conceal a target of interest, especially near the wall.

As a result of the study of wave propagation through walls, we have chosen for the radar transmission a wide frequency band ranging from 1 to 4 GHz. In addition to wall transmission mitigation, this choice is also motivated by increasing the space resolution a way towards ultraresolution imaging and the fight against multipath in indoor.

3. Human Radar Signature

In order to compute the radar power budget, one needs to evaluate the radar cross-section (RCS) of human beings. Thus, we have measured the backscattering of the human body according to the frequency from 2 to 5 GHz. In order to create a database, the RCS of several people from our laboratory has been measured in different attitudes (standing, raised arms, and squatting) in an anechoic chamber. These measurements can learn about human RCS.

In Figure 6, the RCS of two very different standing persons is presented. The first person is a man that measures 1.85 m and weighs 78 kg. The second one is a woman that measures 1.57 m and weighs 45 kg. One can see that the RCS increases with respect to the frequency and varies from one person to another. Nevertheless, the human RCS ranges generally from −8 dBm^2 to 5 dBm^2 over the 2–5 GHz frequency range.

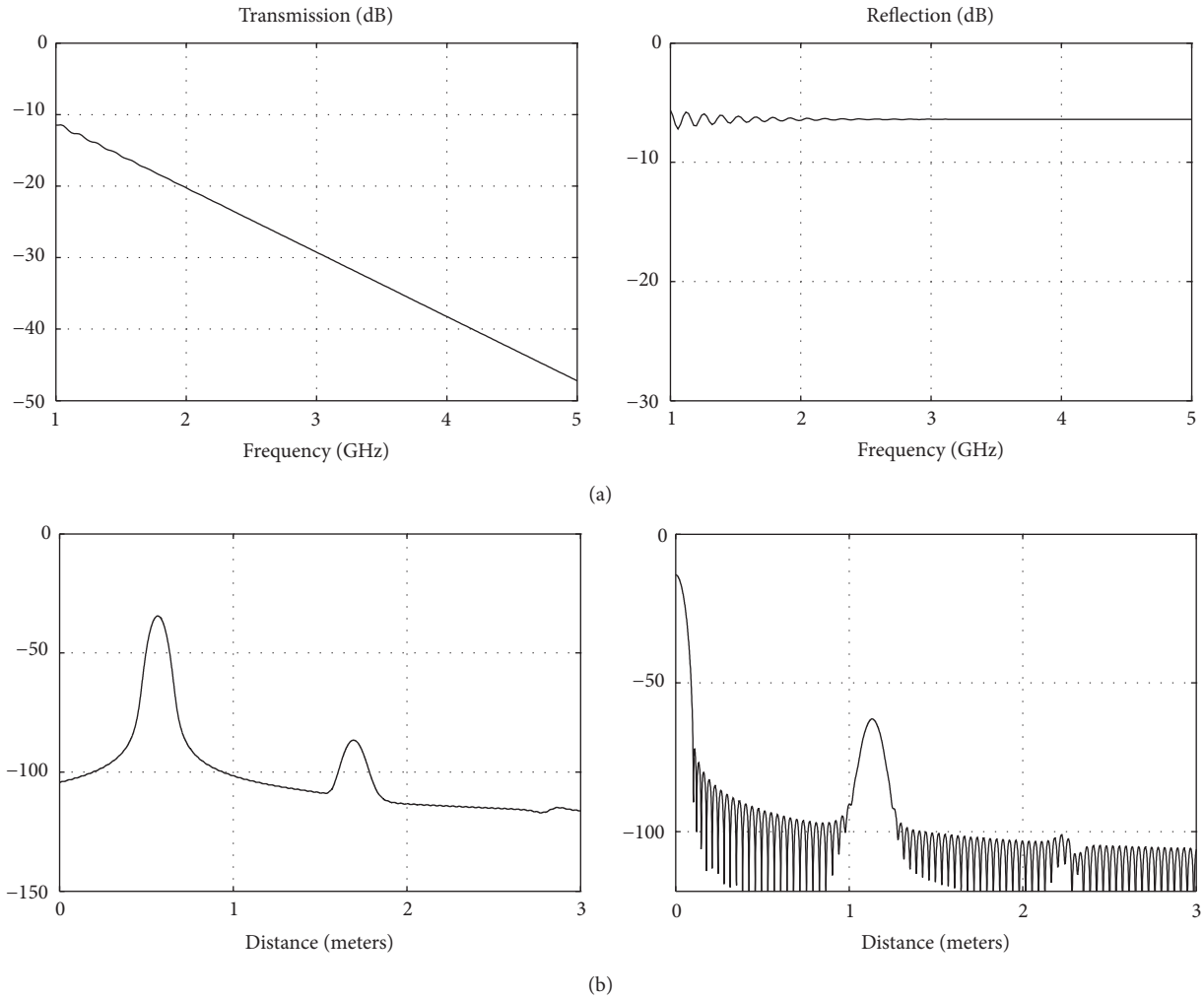

Figure 2: 20 cm solid concrete transmission and reflection coefficient in frequency domain (a) and in time domain (b).

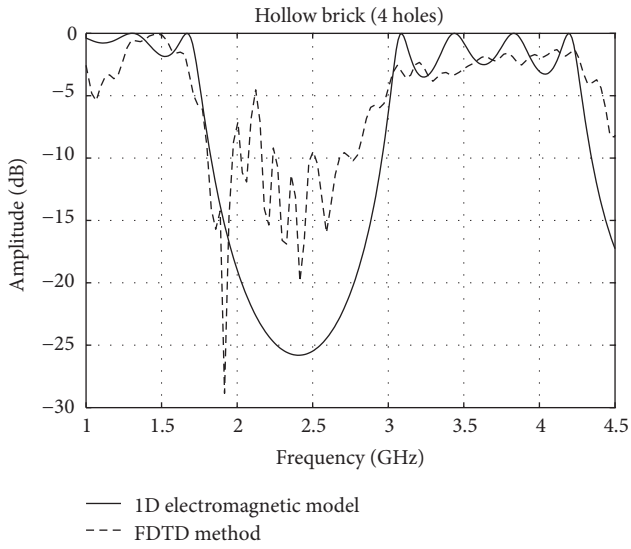

Figure 3: Transmission coefficient comparison between 1D electromagnetic model and FDTD model.

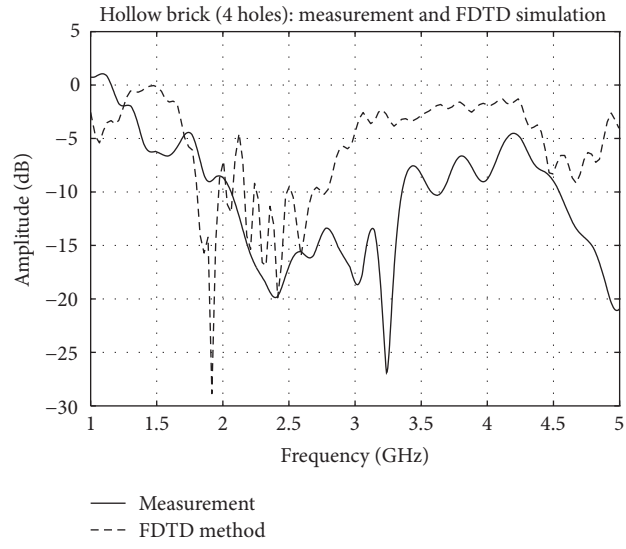

Figure 4: Comparison of transmission coefficient obtained by measurement (full line curve) and by simulation (dashed curve).

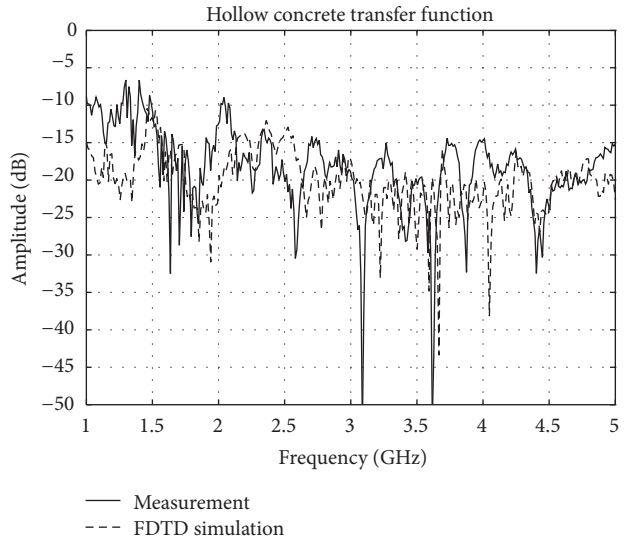

Figure 5: Cinder blocks wall transfer function obtained by measurement and by FDTD simulation.

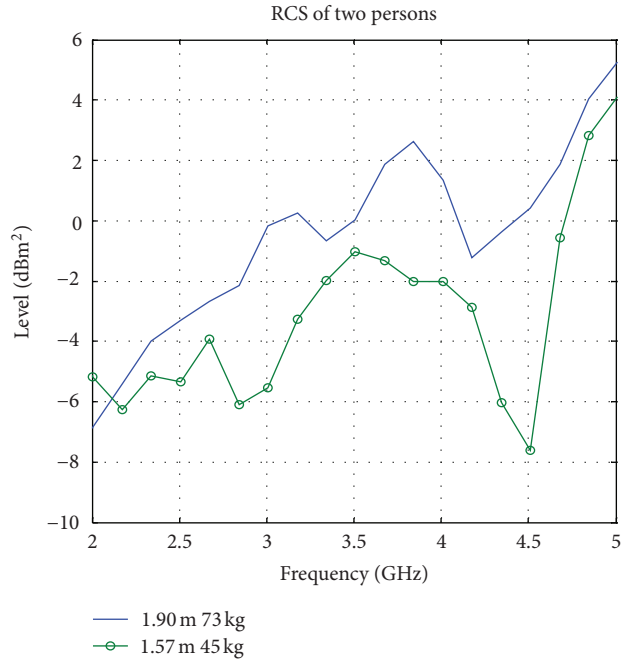

Figure 6: Radar cross-section of two different persons.

4. Technical Considerations for the Conception of TTW Radar

When designing the through-the-wall radar system we had to make some tradeoffs between features such as system complexity (sensor dimension and topology), radar space resolution, time resolution, central frequency, frequency bandwidth, and detection range.

4.1. System Complexity and Topology. System dimension is directly correlated with the level of information the system shall deliver. Two-dimensional radar systems provide a high level of information. Actually, good spatial localization is enabled with this kind of radar system. Antennas are, in this case, gathered in a one-dimensional array. A higher level of information could be delivered by a three-dimensional system which would provide additional knowledge about the volume of targets. This would help to discriminate between different types of targets and also between different human behaviours. However, the use of 3D radars greatly increases the system design complexity. Sensor antenna array must be a surface array and, thus, portability is questionable. It is also questionable for the moment to quickly address an antenna surface array. Besides, the amount of data to process is greatly increased.

Concerning the stand-off radar distance, we have chosen to focus only on short range radar (less that 10 m range). In this case, the sensor is generally hand held and it illuminates only a part of a room. For TTW applications, the short range radar will be useful if the operator can operate safely at low standoff from the building.

4.2. Resolution. Range resolution is ruled by the frequency bandwidth B. Here, a range resolution of about 50 cm seems to be enough in order to discriminate between two persons. Thus, considering this criterion, 300 MHz of useful bandwidth would be a priori sufficient according to the resolution criterion.

Radar cross-range resolution is given by the width of its main lobe:

$$\Delta_a = 2R \cdot t_g\left(\frac{\theta}{2}\right), \tag{2}$$

where R is the distance between the antenna and the target and θ is the antenna main lobe width. Again, for this application, the expected cross-range resolution is about 50 cm. Thus, when the target is at 4 m from the antenna, this criterion would fix antenna main lobe width to about 7°.

4.3. Human Target. Human body can be characterized by its RCS and by its motion. Measurements presented previously have shown that human RCS value lies between −8 and 5 dBm^2. Human motion could be classified depending on the frequency as follow:

(i) macromovements: those concerning a displacement of at least 10 cm ($\approx \lambda$ at 3 GHz) like, for example, a walking displacement (legs or arms movement),

(ii) micromovements: those concerning a displacement of less than 10 cm like, for example, heart beat and breathing movements.

From a radar point of view, these movements could help to ascertain the radar integration time that contributes in improving the signal-to-noise ratio. Integration time T_{int} is here limited by four factors:

(i) the maximum human walk velocity $v_{\mathrm{w\_max}}$;

(ii) the maximum human velocity (internal motion) which brings additive Doppler noise. Let us call the maximum motion velocity $v_{\mathrm{motion\_max}}$;

(iii) the frequency bandwidth B;

(iv) The maximum frequency $f_{\max}$.

The criterion that the target stays inside a cell range of $\Delta R/4$ during T_{int} can be stated as

$$T_{\text{int}}\ v_{\text{w\_max}} \leq \frac{\Delta R}{4}. \tag{3}$$

If we assume a maximum human speed $v_{\text{w\_max}}$ of 3.5 m/s and $\Delta R = 50$ cm, then the observation time should be limited to 40 ms. Another criterion is related to Doppler noise added by the motion of the human body. This motion can lead to failures in pulse compression. One can state that the body parts must not move of more than a quarter of a wavelength during the time T_{int}. This criterion gives a second relation to fulfil:

$$T_{\text{int}} \leq \frac{c}{4 f_{\text{moy}} v_{\text{motion\_max}}}. \tag{4}$$

That is, for $v_{\text{motion\_max}} = 1$ m/s, the observation time should be less than 39 ms at 2 GHz.

4.4. Frequency Tradeoff. Transmission measurement through different types of walls has shown that transmission is different according to the type of walls. In the case of thick walls, especially concrete walls, the attenuation can be very important (up to 40 dB at 4 GHz).

Thus, we have chosen to restrict the frequency range of the TTW radar to the upper part of the UHF spectrum (1 GHz–4 GHz). Frequencies less than 1 GHz would lead to large antenna sizes and arrays. Thus, our device frequency bandwidth is indeed 1–4 GHz.

4.5. Radar Detection Range. It is of utmost importance to evaluate the average power that the system would have to transmit for detecting human targets through walls, according to the desired range.

For this purpose, radar equation is driven by the following relationship between

(i) the minimum received signal power for a target (P_m) based on radar parameters, wavelength (λ), and range (R)

(ii) and the radar sensitivity expressed in terms of the equivalent system temperature and the given signal-to-noise ratio to detect target:

$$P_m \frac{G_T G_R \lambda^2 \sigma T_{\text{obs}}}{(4\pi)^3 R^4 L_S L_m^2} = \text{SNR}_{\min} k_B T_0 F, \tag{5}$$

where

(i) G_T and G_R are antenna gain, respectively, for the transceiver and for the receiver;

(ii) L_S represents the system losses and L_m represents the propagation losses through walls;

Table 1: Radar parameters.

Parameter	Value
System parameters	
Antenna gain ($G_R = G_T$)	5 dB
System losses (L_S)	15 dB
Signal-to-noise ratio ($\text{SNR}_{\min}$)	13 dB
Noise factor (F)	7 dB
Receptor bandwidth	200 kHz
Human beings and walls parameters	
Human RCS (σ)	$(-5, 8)$ dBm^2
Observation time (T_{obs})	40 ms
Wall attenuation	(16, 26) dB

(iii) $k_B T_0 = -114$ dBm/MHz (T_0 is the ambient temperature);

(iv) F is receiver noise factor.

Tables 1 and 2 summarize radar parameters and some assumptions on wall attenuation and human RCS (discussed in the previous sections).

The choice of transmitted power is based on the detection range that the system shall achieve as required by each application. The following table presents the required transmitted power for two ranges: very short-range radar (3 m) and short-range radar (8 m). Two types of walls have been considered. The first one has a low EM attenuation while the second one a much larger one. Wall characteristics are given for a 2 GHz central frequency.

5. UWB FMCW Radar Design

Different technologies are candidate to equip a UWB TTW radar. The FMCW radar is a cost effective solution to high resolution radar. Because it achieves digitally the pulse compression process, its main benefit is to provide a better power budget than the pulsed radar. Namely, the chirp waveform provides the best signal-to-noise ratio. The key point is that, by adjusting the frequency sweeping time in the range of some milliseconds, we can optimize the received electromagnetic energy compatible with the target stationary time.

Our TTW FMCW radar is composed of three main parts communicating between them:

(i) microwave module,

(ii) switched antenna array,

(iii) data acquisition and processing.

The frequency swept is provided by a Yttrium Iron Garnet (YIG) oscillator. At the output, a 10 dB ultrawide band coupler is used to provide the local oscillator signal mixer from the transmitted wave. Received signal is amplified before getting mixed with the reference signal. Beat signal is filtered in order to eliminate the spurious beat frequencies that are due to antennas direct coupling and the return of the wall. On receive, an array of 16 ETSA [8] antennas (exponentially tapered slot antenna) is used. These antennas are

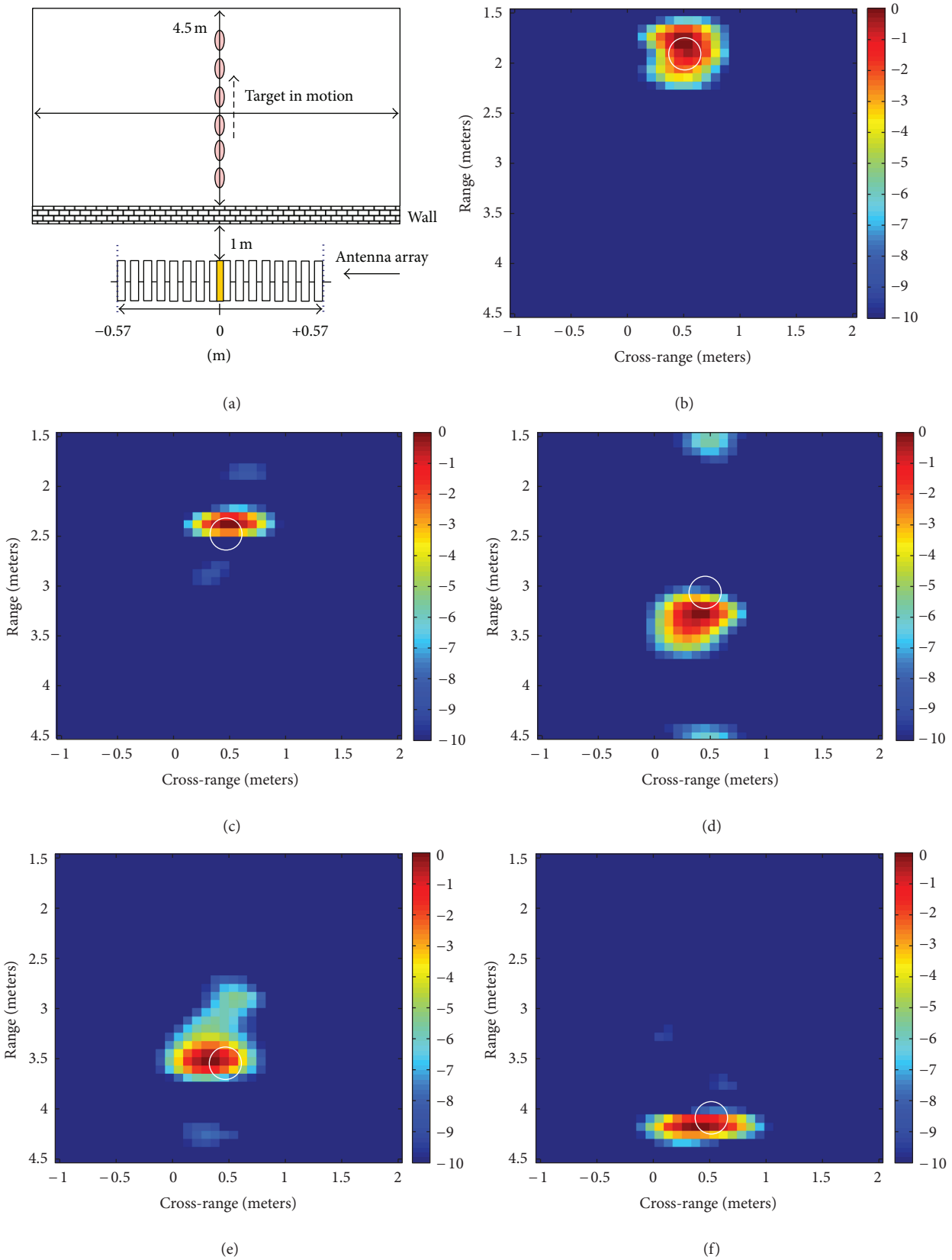

Figure 7: Experimental through-the-wall imaging result.

Table 2: Detection range versus transmitted power.

	Ultrashort-range radar (3 m)		Short-range radar (8 m)	
	Low attenuation	Strong attenuation	Low attenuation	Strong attenuation
Transmitted power (dBm)	3	23	20	40

designed and developed by the LEAT laboratory (Laboratoire d'Electronique Antennes et Télécommunications, Université de Nice-Sophia Antipolis, CNRS UMR 6071). They present a typical 1.2 : 1 VSWR and have a gain of about 10 dB between 1 and 4 GHz. The spacing between the antennas is 7.5 cm. For this distance, direct coupling between antennas is less than 15 dB under the radiated value.

Signal acquisition is achieved by a 3 MS/s 14 bits analog to digital converter from the National Instrument (PXI 6534 board). Data are then processed in real time on a laptop. For each 16 data block (corresponding to the 16 antennas on receive), a special beam forming algorithm that operates in real time is applied in order to obtain a 2D radar image of the observed scene. Fundamentals of digital beam forming are rather well known [9]. Algorithms have also been developed and presented in [10]. Nevertheless, one must apply it here in the special context of through wall imaging [3], with UWB transmission, near-field effects, and through-wall compensation. We have selected the following algorithm (6) for the digital beam former which is very efficient in terms of computation speed.

Let S be the received signal for each frequency F_i and each position of the transmitter $\overrightarrow{r}_T$ and the receiver $\overrightarrow{r}_R$. First the signal is filtered with a time gate Δt around the expected delay. For each position on a grid $\vec{r}$, the local reflectivity η can be computed by summing as follows [11]:

$$\eta(\vec{r}) = \sum_{F_i}\sum_{T}\sum_{R} S\left(F_i, \overrightarrow{r}_T, \overrightarrow{r}_R\right)_{t\in\Delta t} \left|\vec{r} - \overrightarrow{r}_T\right| \left|\vec{r} - \overrightarrow{r}_R\right| \times A\left(F, \vec{k}\right) e^{jk[d(r,r_T,r_R,F)+d_{\text{wall}}]}. \quad (6)$$

In this formula, the distances d depending on $\vec{r}$, $\overrightarrow{r}_T$, and $\overrightarrow{r}_R$ can be computed in advance and stored in a memory in order to avoid calculating it at each iteration. An additional distance that takes into account the wall can be added if one knows the nature and the thickness of the wall (e.g., concrete). For cinder blocks, this correction can be omitted because they contain mainly air inside. The amplitude function A is an antenna dependant function which is a function of the wave number $\vec{k}$ and the frequency. It corrects for the antenna pattern and its dependence in frequency. It includes also the weighting function in frequency and azimuth in order to decrease the side lobes level (like the Hamming's function).

After beam forming, a special image processing that operates a difference between two images recorded close in time has been implemented. As already said, the idea is the elimination of the stationary part of environment and the conservation of the moving target.

6. Experimental Assessments

Measurements in realistic conditions were conducted for radar assessment. The scenario depicts a person walking behind a cinder-block wall. This person is moving away from the wall. Figure 7(a) shows the measurement configuration. Images from Figures 7(b) to 7(f) present the radar images computed by the radar processor at successive instants separated from 0.3 s. White circles pinpoint the real position of the person. The image scale is in dB below the founded maximum value. These results show clearly the radar capability in terms of localization of a person through a cinder-block wall.

7. Conclusion

In this study, a new TTW imaging radar demonstrator using a UWB/FM-CW waveform has been presented and discussed. It is a good candidate for the detection of human beings in motion in a room. The joint use of frequencies in L band and S band meets all the wall case. The UWB waveform provides in essence range resolution and wall transmission mitigation. By using an array of UWB antennas, one can localize a target by digital beam forming on receive. This TTW radar concept has been demonstrated by a successful trial.

Acknowledgment

A part of this study has been supported by the DGA in the framework of a Ph.D. thesis.

References

[1] L. M. Frazier, "Surveillance through walls and other opaque materials," *IEEE Aerospace and Electronic Systems Magazine*, vol. 11, no. 10, pp. 6–9, 1996.

[2] G. Barrie, "Ultra-wideband synthetic aperture, data and image processing," Technical Memorandum DRDC Ottawa TM 2003-015, 2003.

[3] F. Ahmad, M. G. Amin, and S. A. Kassam, "Synthetic aperture beamformer for imaging through a dielectric wall," *IEEE Transactions on Aerospace and Electronic Systems*, vol. 41, no. 1, pp. 271–283, 2005.

[4] N. Maaref, P. Millot, C. Pichot, and O. Picon, "A study of UWB FM-CW radar for the detection of human beings in motion inside a building," *IEEE Transactions on Geoscience and Remote Sensing*, vol. 47, no. 5, pp. 1297–1300, 2009.

[5] D. I. Axiotis and M. E. Theologou, "2 GHz outdoor to indoor propagation at high elevation angles," in *Proceedings of the 13th IEEE International Symposium on Personal, Indoor and Mobile Radio Communications (PIMRC '02)*, vol. 2, pp. 901–905, September 2002.

[6] G. Klysz, J. P. Balayssac, and X. Ferrières, "Evaluation of dielectric properties of concrete by a numerical FDTD model

of a GPR coupled antenna—parametric study," *NDT & E International*, vol. 41, no. 8, pp. 621–631, 2008.

[7] A. Tavlove, *Advances in Computational Electrodynamics: the Finite Difference Time-Domain Method*, Artech House, 1998.

[8] E. Guillanton, J. Y. Dauvignac, C. Pichot, and J. Cashman, "A new design tapered slot antenna for ultra-wideband applications," *Microwave and Optical Technology Letters*, vol. 19, no. 4, pp. 286–289, 1998.

[9] B. D. Van Veen and K. M. Buckley, "Beamforming: a versatile approach to spatial filtering," *IEEE ASSP Magazine*, vol. 5, no. 2, pp. 4–24, 1988.

[10] M. Soumekh, *Synthetic Aperture Radar Signal Processing with MATLAB Algorithms*, John Wiley & Sons, 1999.

[11] N. Maaref, P. Millot, C. Pichot, and O. Picon, "Through-the-wall radar using multiple UWB antennas," in *Proceedings of IET International Conference on Radar Systems (RADAR '07)*, pp. 40–41, Edinburg, UK, October 2007.